Pis'ma v ZhETF, vol. 88, iss. 9, pp. 712 – 716

The Fermi surface reconstruction in stripe phases of cuprates

M. Ya. Ovchinnikova[1)]

N.N.Semenov Institute of Chemical Physics RAS, 117334 Moscow, Russia

Submitted 25 July 2008
Resubmitted 19 September 2008

Mean-field study of the stripe structures is conducted for a hole-doped Hubbard model. For bond-directed stripes, the Fermi surface consists of segments of an open surface and the boundaries of the hole pockets which appear in the diagonal region of momenta under certain conditions. Segments of the first type are due to one-dimensional bands of states localized on the domain walls. The relation of bands to the doping and temperature dependences of the Hall constant is discussed. In connection with the observation of quantum magnetic oscillations, a systematic search for the electron pockets has been carried out. It is shown that the formation of such pockets in bilayer models is quite possible.

PACS: 71.10.Fd, 74.20.−z

Numerous properties of underdoped (UD) cuprates are connected with the formation of stripes – the periodic spin and charge structures specified from the positions of magnetic peaks in neutron scattering [1]. New impetus to a discussion of the normal state properties has been given by the measurements of longitudinal and Hall conductivities of cuprates in strong magnetic fields suppressing the superconductivity. A change of sign of the Hall coefficient R_H as $T \to 0$ in the Y- and La-based cuprates [2, 3] and magnetic quantum oscillations of R_H, magnetization and conductivity have been revealed in $YBa_2Cu_3O_{6+y}$ (Y123) and $YBa_2Cu_4O_8$ (Y124) compounds [2, 4, 5].

The observations testify to a reconstruction of the Fermi surface (FS). The temperature of its onset is associated with the start of deviations of resistivities and the Hall coefficient $R_H(T)$ from a linear T-dependence typical for large T. There are two doping regions in UD cuprates with different signs of the deviations. First doping region near an optimal doping reveals itself in a sharp increase of positive $R_H(T)$ for $T < T^*$ in $La_{1-x}Sr_xCu_4$ (LSCO) [6]. Such behavior may be due to the transition from paramagnetic normal state with a large FS to the state with some charge-spin structure exemplified by dividing the large FS into arcs of the hole pockets. In the region of small doping, the $R_H(T)$ falls down for $T < T^*$ and becomes negative as $T \to 0$. This might be connected with changes in the charge and spin stripes, which are most evident near the temperature T_s of the structural LTO $\to$ LTT transition between low-temperature orthorhombic (LTO) and low-temperature tetragonal (LTT) phases.

To explain the negative sign and quantum oscillations of R_H as $T \to 0$, it was supposed that an opening of the electron (e-) pockets in FS occurs [4, 5]. Then a question may be posed: can the stripe phases give rise to such a sort of FS segments? In principle, work [7] confirms such a possibility. But it leans upon a very rough model in which the stripe impact on electronic states is described by an outer periodic potential. According to other hypothesis [8, 9] the e- and h-pockets arise from a d-density wave order (DDW) of the normal state. This is a state with the alternating orbital currents predicted in the models with a sufficiently strong electron interaction of the neighbor sites. There is no yet an experimental confirmation for the DDW order, unlike the stripes. Nevertheless, in principle, such order might give rise to e-pockets, and the incommensurate DDW – to a set of the pockets and frequencies of the magnetic quantum oscillations. The DDW state in [8, 9] is described by the lowest harmonics of the fixed non-self-consistent current's fields.

As distinct from two Hubbard bands of a homogeneous antiferromagnetic state, a periodic structure with n_c sites in a unit cell is characterized by n_c bands. Their sections at the Fermi level provide the FS segments of different types. To study them, one must be convinced of the stripe formation and determine the self-consistent periodic potential including all harmonics.

In the present work, the mean field (MF) approximation is used to study the bands and the FSs of periodic stripe structures in the t-t'-t"-U Hubbard models. The early studies of stripes [10, 1] had shown that the doped holes are localized mainly on domain walls (DWs). The stripes provide also an explanation [11 – 13] for the observed fragmentation of FSs and dichotomy of the nodal

[1)] e-mail: movchin@chph.ras.ru

and antinodal quasiparticles. Here we extend the calculations to a more wide set of structures with the systematic search for electronic pockets among the FS segments.

The zero band of the model is taken in the form $\epsilon(k) = -2t(c_x + c_y) + 4t'c_xc_y - 4t''(c_x^2 + c_y^2 - 1)$, where $c_{x(y)} = \cos[k_{x(y)}]$. The on-site repulsion and positive values of intersite hopping at the distances a, $\sqrt{2}a$, $2a$ (a is the lattice constant) are equal to

$$U/t = 4, \quad t'/t = 0.3, \quad t''/t' = 0.5. \tag{1}$$

Our calculations will cover the doping range with $x > 0.05$ and the structures S_l or B_l with the DWs directed along the y-bonds and centered at the sites or the bonds, respectively. The stripe period, i.e., the distance between DWs l (in units of a) is varied in the range $l = 7 \div 4$. This range corresponds to the observed linear doping dependence of the incommensurability parameter $\delta = 1/2l = x$ for $x \leq 1/8$ and its saturation value $\delta = 1/8$ for $x > 1/8$. The direct and reciprocal lattice vectors of the structure are $E_{1,2} = (la, \pm a)$, $B_{1,2} = \frac{\pi}{a}(\frac{1}{l}, \pm 1)$ or $E_1 = (la, 0)$, $E_2 = (0, 2a)$, $B_1 = (2\pi/la, 0)$, $B_2 = (0, \pi/a)$ at even l or odd l, respectively. A number of sites in a unit cell equals $n_c = 2l$.

The order parameters of a periodic MF solution are represented by the charge and spin densities at the sites of a unit cell. The MF procedure was described in Refs. [11, 13]. One-particle states

$$\chi^\dagger_{\tilde{k}\nu} = \sum_{m,\sigma} c^\dagger_{k_m,\sigma} W_{m\sigma,\nu}(\tilde{k}) \tag{2}$$

are the eigenstates of a linearized Hamiltonian. They determine the spin-degenerate bands $E_\nu(\tilde{k})$ ($\nu = 1, \ldots n_c$) of the periodic structure. Here $k_m = \tilde{k} + Bm$, $Bm = B_1m_1 + B_2m_2$, $\tilde{k}$ runs over momenta in a reduced Brillouin zone (BZ) of the structure, and $m = (m_1, m_2)$ numerates all independent Umklapp vectors. The $E_\nu(k)$ bands, the W matrix in formula (2) and the Fermi function $f(\omega)$ determine the spectral density $A(k, \omega)$ and the photoemission intensity $I(k, \omega)$:

$$\begin{gathered} I(k,\omega) \sim A(k,\omega) f(\omega), \\ A(k,\omega) = \textstyle\sum_{m,\nu,\sigma} |W_{m\sigma,\nu}|^2 \tilde{\delta}(E_\nu(k_m) - \mu - \omega). \end{gathered} \tag{3}$$

A density map of function (3) at $\omega = 0$ visualizes the main and shadow segments of the FS. A density map of the local (in k-space) density of states, viz.

$$D(k,\omega) = \sum_\nu \tilde{\delta}(E_{k,\nu} - \mu - \omega), \tag{4}$$

allows us to overview full sections of bands at the level $E = \mu + \omega$ regardless of their weights in photoemission. Here, $\tilde{\delta}$ in Eqs (3),(4) is the delta-function with some finite width which was taken $\sim (0.02 \div 0.04)t$ by order of magnitude.

Fig.1 presents typical FSs and their 'visible' segments for the S_4 structure at doping $x = 0.15$. It has

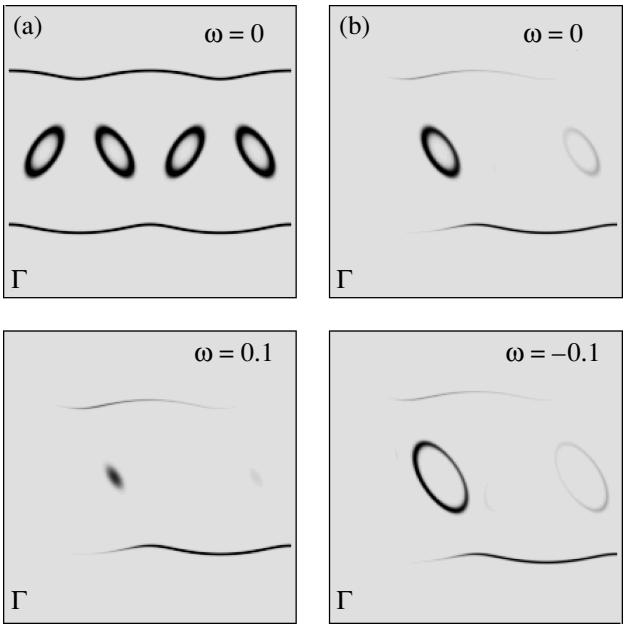

Fig.1. Fermi surfaces and their 'visible' segments for the S_4 structure with $l = 4$ at doping $x = 0.15$ on the density maps of (a) the local density of states $D(k, \omega = 0)$, and (b) the spectral function $A(k, \omega = 0)$ in the first quadrant of a Brilluoin zone. Low panels: the density maps of $A(k, \omega)$ at $\omega = \pm 0.1$ (in units of t)

been checked that the open FSs give rise to quasi-one-dimensional (1D) bands of states localized on the domain walls. Localization of the 1D states on the DWs had been proved [14] by a narrow distribution of their amplitudes over the sites near DWs. Small width of the distribution means a participation of several (not one) harmonics generated by the stripes in the self-consistent linearized hamiltonian. Closed segments of FSs represent the boundaries of the hole pockets. A decrease in doping leads to narrowing the h-pocket. It is clearly seen from the maps of the spectral function at $\omega \neq 0$ in Fig.1. For the same S_4 structures, the hole pockets disappear for $x < x_{arc} = 0.135$ and only 1D FS segments retain. Similar behavior is displayed by the B_4 structure.

The 1D bands with a full suppress of photoemission from the nodal region have been observed in $La_{1.28}Nd_{0.6}Sr_{0.12}CuO_4$ compound [15] in which the static stripes have been revealed. The temperature and

doping dependences of the Hall constant have been explained [16] by a crossover from the 2D to 1D type electronic structure which occurs with disappearing the h-pockets.

Fig.2 depicts the energies $[E_\nu(k_x, k_y) - \mu]$ of bands $\nu = 3, 4, 5$ closest to the Fermi level μ for the S_4 model

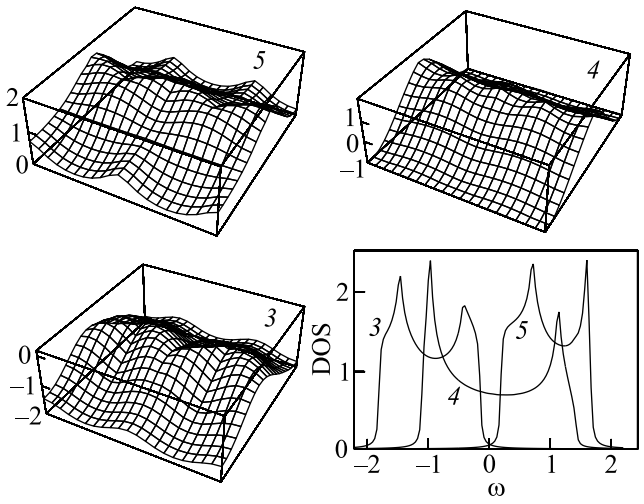

Fig.2. Energies $[E_\nu(k) - \mu]$ for bands $\nu = 3, 4, 5$ of the S_4 structure at doping $x = 1/8$ in the first quadrant of BZ. Right bottom: the $\mathrm{DOS}_\nu(\omega)$ contributions from the same bands into the density of states (per one unit cell). The band numbers ν mark the graphics and curves. The energies and ω are given in units of t

at doping $x = 1/8$. Numbering of bands is made in increasing order of their energies. Band $\nu = 3$ is close to touch the Fermi level from below and, consequently, it is responsible for the hole pockets at higher doping. Band $\nu = l = 4$ is the 1D band with an open FS. And the band $\nu = 5$ approaches the Fermi level from above at the points $k = (0, \pi) + B_i m_i$. Decrease of doping at the fixed stripe period l would led to the appearance of electronic pockets. But in reality it is accompanied by a change in the stripe period l according to $\bar{l}(x) \sim 1/2x$ at low T and $x < 1/8$. Characteristic cyclotron masses m_1 and m_2 of the h- or e-carriers in the case of opening the corresponding h- or e-pockets or during their activation depend only slightly on doping and are of order $m_1 \sim 0.41 m_e$, and $m_2 \sim 0.92 m_e$ (m_e is the electron mass).

Notice that the self-organized stripes lead to formation of some gap in the density of states $\mathrm{DOS}(\omega)$ of the system at the Fermi level. It is not a full gap $[\mathrm{DOS}(\omega = 0) \neq 0]$. But such a gap is absent in the homogeneous antiferromagnetic state of model (1): contributions to the $\mathrm{DOS}(\omega)$ from upper and lower Hubbard bands are overlapping. Situation is similar to that in semiconductors where the self-organized charge distribution among impurities provides a gap in DOS at the Fermi level.

Thus, the S_l, B_l structures with the period $l = 5, 6, 7$ correspond to doping range $0.05 \leq x \leq 0.125$ at small T. At doping $x_l = 1/2l$ there are only 1D segments of the FS. The hole pockets and nodal Fermi arcs are absent, though the system is close to their opening. Variations in the temperature for the fixed structure change only slightly the bands and FSs of the MF solutions. Therefore, the observed temperature dependences of the Hall constant and the length of the small Fermi arc cannot be explained in the context of a fixed structure. They may be understood if one infers a change in structure with increasing T, for example, a growth of the average stripe period with T. The growth of $\bar{l}(T)$ decreases a density of domain walls and a concentration of holes localized on them. At fixed doping, this is accompanied by the opening of the h-pockets, increase of the Fermi-arc length, and growth of the positive (hole) contribution to the Hall constant. Hypothesis for the T-dependent $\bar{l}$ is in accordance with the observed temperature dependence of the incommensurability parameter, which shows up more explicitly in the region near a transition from tetragonal to orthorhombic (LLT $\rightarrow$ LTO) phases in $La_{2-x}Ba_xCuO_4$ [17] at doping $x = 1/8$.

It should be noted that the quasi-1D FS segments in LSCO (unlike NLSCO) are not observed in the angle-resolved photoemission spectra (ARPES) [18]. This may be connected with the irregular stripes, inhomogeneity and multi-structure nature of LSCO.

The results obtained for periodic structures may be usefull in interpreting the two-component character of the effective concentration $n_H(x, T)$ of the Hall carriers [19]. Its doping and temperature dependences have the following form [19–21]

$$n_H = n_0(x) + n_1(x) \exp[-E(x)/kT]. \qquad (5)$$

Concentration $n_0(x) = x$ of the first type carriers which survive as $T \rightarrow 0$ coincides with the concentration $n_h = 1/2l = x$ of holes localized on the domain walls if the hole pockets have not yet opened (for $x < x_{arc}$). The second type carriers in formula (5) may originate from the activation of holes in the nodal region before the opening of the hole pockets at small T and x. At large T, after the opening of h-pockets, these carriers might originate from a large Fermi arc including the antinodal regions of the van-Hove singularity which resides below the Fermi level in UD cuprates.

The monolayer models studied above do not display the electron pockets. A decrease in the most crucial parameter t'/t down to the value $t'/t = 0.2$ strongly increases the activation energy for quasiparticles from the

potential e-pockets: the gap between a quasi-1D band $\nu = l$ and next upper band $\nu = l+1$ for the S_l, B_l structures sharply increases with a decrease in t'/t. The 1D bands may provide the negative contribution to the Hall conductivity σ_H. This was confirmed by calculations of the 1D band contribution in a first approximation with respect to the overlapping between the states localized on the neighboring domain walls. The estimates have been made in the context of hopping mechanism of conductivity, which is suitable at small T. In case of coherent transport accross the stripes one needs a further study of possible responsibility of 1D bands for the magnetic quantum oscillaions.

Taking into account the above reasoning we remind that quantum oscillations have been observed in the bilayer cuprates, viz. in the ortho-II Y123 and Y124 [4, 5]. Therefore, we have calculated the FSs and bands of stripes in bilayer models. Interlayer interaction is then described by a splitting $\Delta = t_z(\cos k_x - \cos k_y)^2/2$ of the zero bands in the standard form [22]. Fig.3 presents the FSs for bilayer model with the parameters entering

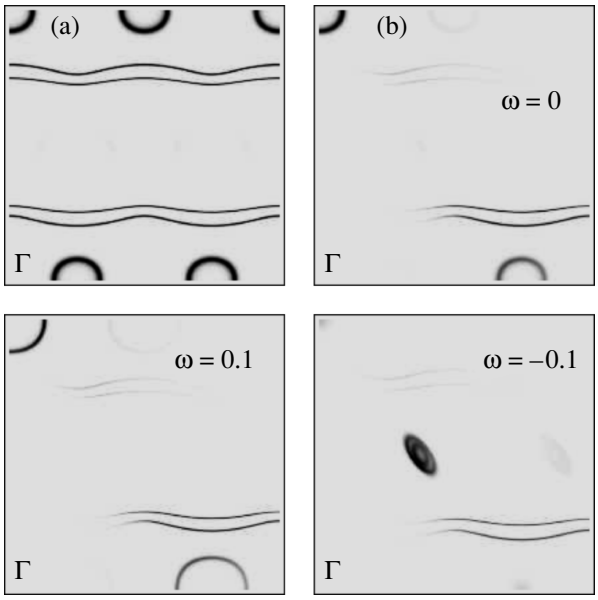

Fig.3. Fermi surfaces and their 'visible' segments on the maps of the local density of states $D(k, \omega = 0)$ and the spectral density $A_\Sigma(k, \omega = 0)$ for bilayer model with parameters (1), $t_z = 0.35t$ and the stripe structure S_4 in each layer. Lower panels: the maps of $A_\Sigma(k, \omega)$ at $\omega = \pm 0.1t$ demonstrate evolution of e- and h-pockets. All maps are given in I quadrant of BZ at doping 0.125

Eq. (1) and $t_z/t = 0.35$, and synchronized antiphase stripe structures in both layers ($S_{zn1} = -S_{zn2}$ in the layers 1,2). A map of the summary local density of states $D_\Sigma(k, \omega)$ and the spectral function $A_\Sigma(k, \omega) = A_+(k, \omega) + A_-(k, \omega)$ from the bonding and antibonding bands (BB and AB, respectively) are given at doping $x = 0.125$. For the stripes directed along y, the e-pockets are seen at the points $(0, \pi) + B_i m_i$ in addition to the split open FS segments of 1D bands. The boundaries of the e-pockets around $(0, \pm\pi)$ display the maximum photoemission intensity, and they correspond to BB bands. The electronic nature of these pockets (unlike the nodal hole pockets) is proved by their evolution with ω on the map $A_\Sigma(k, \omega)$ (Fig.3). Although the zero band bilayer splitting goes to zero in the nodal lines, despite that the bilayer splitting of the 1D bands is only slightly dependent on the direction of the vector $[k - (\pi, \pi)]$ for k moving along FSs of these bands. The area of electronic pocket represents about 1.1% of the magnetic Brillouin zone area. The order of magnitude of this value does not contradict to the estimate of 2.3% obtained from the observed frequency of quantum magnetic oscillations.

In summary, the MF calculations of the stripe structures in UD Hubbard model reveal two types of the Fermi surface segments: segments of open FSs from the 1D bands, and closed boundaries around the hole pockets in the nodal region. First type carriers with the concentration linear in doping refer to states localized on the domain walls and provide the quasi-1D charge transport. For the observed relation $x = 1/2\bar{l}(x) \leq 1/8$ between doping and the stripe period only the first type carriers survive as $T \to 0$ with a small contribution from activated hole carriers. Increase in the activated hole concentration with increasing T explains the rise of R_H from negative to positive values if one infers the growth of the stripe period with T. Negative R_H as $T \to 0$ might be caused by hoping conductivity of the 1D carriers. But quantum oscillations can only be explained by the appearance of e-pockets. In monolayer models, the search for them fails. But the bilayer striped models exhibit the opening of electronic pockets in antinodal regions for bonding bands. These e-pockets might be responsible for magnetic quantum oscillations in YBCO. Though the results are sensitive to values of the model parameters, nevertheless the MF calculations allow to conclude the following. 1)The simultaneous opening of the e- and h- pockets in the self-organized stripe structures is unlikely. 2) The quasi-1D bands with open FS and their partial occupation should be taken into account in the whole charge balance in discussion of the revealed multi-harmonic magnetic oscillations in YBCO [23, 24].

1. S. A. Kivelson, I. P. Bindloss, E. Fradkin et al., Rev. Mod. Phys. **75**, 1201 (2003).

2. T. Adachi, T. Noji, and V. Koike, Phys. Rev. B **64**, 144524 (2001).
3. D. LeBoeuf, N. Doiron-Leyraud, J. Levallois et al., Nature, **450**, 533 (2007).
4. F. F. Balakirev, J. B. Betts, A. Migliori et al., Nature **424**, 912 (2003).
5. N. Doiron-Leyraud, C. Proust, D. LeBoeuf et al., Nature **447**, 565 (2007).
6. R. Daou, D. LeBoeuf, N. Doiron-Leyraud et al., arXiv: cond-mat/0806.2881.
7. A. J. Millis and M. R. Norman, Phys. Rev. B **76**, 220503 (2007).
8. S. Chakravarty and H.-Y. Kee, arXiv: cond-mat/0710.0608v4.
9. I. Dimov, P. Goswami, X. Jia, and S. Chakravarty, arXiv: cond-mat/0807.4202.
10. J. N. Tranquada, H. Woo, T. G. Perring et al., Nature **429**, 531 (2004).
11. M. Ya. Ovchinnikova, Zh.Eksp.Teor.Fiz. **127**, 120 (2005) [JETP **100**, 106 (2005)].
12. M. Granath, Phys. Rev. B **74**, 245112 (2006).
13. M. Ya. Ovchinnikova, Zh.Eksp.Teor.Fiz. **131**, 525 (2007) [JETP **104**, 474 (2007)].
14. M. Bosch and Z. Nussinov, arXiv: cond-mat/0208383v2.
15. T. Noda, H. Eisaki, and S. Uchida, Science **286**, 286 (1999).
16. X. J. Zhou, P. Bogdanov. S. A. Kellar et al., Science **286**, 268 (1999).
17. M. Fujita, H. Goka, K. Yamada et al., Phys. Rev. B **70**, 104517 (2004).
18. T. Yoshida, X. J. Zhou, D. H. Lu et al., J. Phys.: Condens. Matter **19**, 25209 (2007).
19. L. P. Gor'kov and G. B. Teitel'baum, Phys. Rev. Lett. **97**, 247003 (2006).
20. S. Ono, S. Komiya, and Y. Ando, Phys. Rev. B **75**, 024515 (2007).
21. L. P. Gor'kov and G. B. Teitel'baum, arXiv: cond-mat/0803.2275.
22. A. I. Lichtenstein, O. Gunnarson, O. K. Andersen, and R. M. Martin, Phys. Rev. B **54**, 12505 (1999).
23. S. E. Sebastian, N. Harrison, E. Palm et al., Nature **454**, 200 (2008).
24. N. Harrison and S. E. Sebastian, arXiv: cond-mat/0208383.